A method for the preparation of high purity lead titanate zirconate solid solutions by carbonate–gel composite powder precipitation

T. R. Narayanan Kutty and P. Padmini

Materials Research Centre, Indian Institute of Science, Bangalore 560 012, India

A novel wet chemical route for the preparation of perovskite titanates (ABO_3 type, where A is a divalent cation and B is a tetravalent cation) such as $PbTiO_3$ and its solid solutions, is described. The method involves the coprecipitation of the divalent cations (A) as fine particles of carbonates with hydrated gels of titania or zirconia ($BO_2 \cdot xH_2O$, $12 < x < 130$; $B = Ti^{4+}, Zr^{4+}$) by the addition of ammonium carbonate. Such coprecipitation is possible because of the instability of the carbonates and oxycarbonates of Ti and Zr in aqueous media in comparison to the polymerised hydroxides, whereas lead carbonate is precipitated readily. The method gives rise to composite powders in which the submicron crystalline particles of the carbonates, crystalline to X-ray diffraction, are embedded within amorphous gels of $BO_2 \cdot xH_2O$. The composite nature of the precipitate is confirmed by transmission electron microscopy. The precipitate is dried and calcined at elevated temperatures. Upon heating to 350–400 °C, the reaction between the carbonate and the amorphous dry gel proceeds *via* the formation of the intermediate $PbO \cdot zTiO_2$ ($z < 0.09$) solid solution which then converts to a defect pyrochlore phase ($A_2B_2O_{7-\delta}$, $\delta = 1$). Above 450 °C, the latter converts to an isocompositional perovskite phase. The process is superior to ceramic methods because of the high purity, uniform chemical homogeneity and lower particle size of the final product.

The simple ABO_3 perovskite compounds such as $BaTiO_3$, $SrTiO_3$, $PbTiO_3$, $PbZrO_3$ and their solid solutions are archetypal ceramics with a long history of technological applications in the electronics industry.[1] Increasing demands on the quality of electronic ceramics have led to greater sophistication in the processing of these materials at both the powder synthesis stage and subsequent densification to solid components or thin dielectric layers. The growing awareness of the need for scientific elegance in the processing of ceramic powders before firing is clear in much of current emphasis on novel low-temperature synthesis techniques.

Lead titanate has been a very attractive material for many years from both scientific and practical aspects. This material has the highest Curie temperature (490 °C) and the largest anisotropy ($c/a = 1.064$ in the tetragonal phase) in the simple perovskite family. PZT has been attracting the attention of the microelectronics community in recent years owing to its potential applications in non-volatile, radiation-hard, random access memories. It offers high remanent polarisation and sufficiently low coercive field strength. It also finds importance in room temperature operated IR sensors from the viewpoint of their applications such as remote sensing, biomedical thermography, gas detection and alarms.

Various wet chemical routes have been described for the preparation of perovskites.[2] The different processes are listed in Table 1. The selection of the processing method depends to a large extent on the final applications. Understandably, electronic ceramics require raw material powders with much higher purity, better homogeneity and high reactivity.[3] It is well known that the characteristics of the fine powders, such as particle size and shape, point defect contents, microstrain and dislocation distribution, influence the final electrical properties of the ceramics. In this respect, the present route, referred to as carbonate–gel composite powder precipitation, yields high-purity ultrafine powders with predictable dopant levels and a high degree of compositional homogeneity. The peculiarity is that the product on annealing crystallises *via* the formation of an intermediate defect pyrochlore phase which has the same composition as that of the perovskite.

Table 1 Different chemical processes for the preparation of perovskite titanates

sol–gel processing[a]	– mixed alkoxide route
	– carboxy–alkoxide route
	– hydroxide–alkoxide route
hydrothermal synthesis[b]	
synthesis from complex precursors[c]	– oxalate route
	– acetate route
	– citrate route
evaporative decomposition[d]	– liquid mix process
	– spray pyrolysis
ceramic routes[e]	– mixed oxides/solid–solid reaction

[a]Ref. 3, 4. [b]Ref. 5–7. [c]Ref. 8, 9. [d]Ref. 10. [e]Ref. 11.

Experimental

Gels of the hydrated metal hydroxides $B^{n+}(OH)_n$ or $B^{n+}O_{n/2} \cdot xH_2O$ ($B = Ti^{4+}, Zr^{4+}$) were coprecipitated with the carbonates of Pb^{2+} by the addition of ammonium carbonate at 30–40 °C to the corresponding mixed nitrate solutions until pH 6–8. The precipitate was then washed free of the anions and the ammonium ions. The precipitate was finally dried at 120 °C for 12 h and then calcined at elevated temperatures. Calcination at the appropriate temperature is necessary to (i) obtain a stoichiometric crystalline phase, (ii) remove any residual solvent and (iii) obtain powders with the desired agglomerate size, surface area and crystal structure according to the end application. This heat treatment has an important effect on the phase content, microstructure and electrical properties of the ceramics prepared from these powders.

Phase identification of the powders was carried out by X-ray powder diffraction using a Scintag/USA diffractometer using Cu–Kα radiation. For precise lattice parameter measurements, higher angle reflections were chosen. The reflection peaks were recorded at a scanning speed of $0.125^\circ\ min^{-1}$. Electronic-grade silicon was used as an internal standard. Particle size and shape were evaluated by the intercept method on the micrographs from the transmission electron microscope (TEM; JEOL 200 CX, 200 kV) having 2 Å resolution. The chemical composition of the products and the contaminants, if any, were determined by wet chemical analysis using atomic absorption spectroscopy (AAS; Perkin-Elmer 2980). Thermal

analyses were performed on a simultaneous thermogravimetry–differential thermal analysis (TG–DTA) instrument from Polymer Laboratory, STA 1500, at a heating rate of 5–8 °C min^{-1}.

Results and Discussion

The method reported gives rise to composite powders wherein submicron crystalline particles of lead carbonate are embedded within the amorphous gels of titania or zirconia. The carbonates of titanium or zirconium are not formed as they are unstable. Moreover, titanium and zirconium tend to form polymeric chains such as $(Ti–O–Ti)_n$ and $(Zr–O–Zr)_n$ in preference to isolated Ti^{4+} or Zr^{4+} ions. It is well known that independent, hydrated Ti^{4+} in the form of $Ti(OH)_4$ does not exist because of the high charge to ionic radius ratio (5.9 for the six-coordinate ion). In addition, Ti^{4+}, which prefers octahedral coordination, cannot be stabilised by carbonate ligands for steric reasons. Therefore, neither titanium carbonate nor zirconium carbonate is formed from aqueous solutions. Hydrolysed products are produced readily from Ti^{IV} solutions even at intermediate pH ranges. The often proposed $(TiO)^{2+}$ and $(ZrO)^{2+}$ ions are in fact made up of Ti—O—Ti and Zr—O—Zr bridged polymers. Thus the precipitate obtained by increasing the pH of the Ti^{IV} solutions in the presence of ammonium carbonate gives rise to only hydrated titania in the form of a gel. At best, the hydrated oxides thus formed may have partial substitution of the terminal hydroxy groups by carbonate groups.

The metal hydroxide gels are in general polymeric chains forming an entangled network in which the solvent is entrapped. The effective molar volume of this network is very large in comparison to that of lead carbonate, formed simultaneously as crystalline fine particles. As a result of the large difference in the molar volume, lead carbonate becomes embedded within the polymeric network of the gel. This accounts for the generation of the composite precipitate.

Lead titanate ($PbTiO_3$)

TEM studies. The TEM studies clearly illustrate the composite nature of the powder. Fig. 1(a)–(c) shows micrographs of the as-prepared powder of $PbTiO_3$, at different magnifications, showing the titania gel particle with $PbCO_3$ embedded in it. The corresponding electron diffraction pattern [Fig. 1(d)], which shows the spotty pattern superimposed with the haloes, further confirms the presence of two phases in the system, *i.e* TiO_2 as the amorphous phase and $PbCO_3$ as the crystalline phase. The broad haloes seen in Fig. 1(e), for the $PbCO_3$-free gel of hydrated titania precipitated from the ammonium carbonate medium, further supports the presence of an amorphous phase in the system. Furthermore, the powder X-ray diffraction studies show no reflections of TiO_2 (anatase or rutile), indicating that the hydrated titania is X-ray amorphous.

Thermoanalytical studies. The TG–DTA curves of the hydrated titania [Fig. 2(a)] show an endotherm below 100 °C (mass change 16%) and another around 300–320 °C (mass change 17%). The TG curves indicate that essentially all the mass loss in the sample occurred below 400 °C. This mass loss is due to the removal of water from the xerogel. The recrystallisation step has been reported to be above 500 °C for titania gel.[12]

In the TG–DTA curves of $PbCO_3$ [Fig. 2(b)] two endotherms are observed, at 275 °C (mass change 10%) and 330 °C (mass change 6%), corresponding to the decomposition of $PbCO_3$ to PbO in two steps, due to non-equivalent carbonate groups in the crystalline structure. In contrast, the TG–DTA results of the as-prepared carbonate–gel composite powder [(Fig. 2(c)] show the mass loss to occur in three steps: (i) below 100 °C (mass change *ca.* 6%), the mass loss arises from water resorbed by the oven-dried samples when handled in the air, (ii) around 260 °C (mass change *ca.* 4%) corresponding to the decomposition of $PbCO_3$ and (iii) around 300–320 °C (mass change *ca.* 2.5%) due to the reaction of amorphous hydroxylated titania with PbO accompanied by the release of water due to dehydroxylation. There is only minor mass loss above 350 °C (mass change *ca.* 0.5%). The corresponding endothermic maxima are observed around 50, 255 and 300 °C [Fig. 2(c)] in the TG–DTA curves. The change in the course of the $PbCO_3$ decomposition is as a result of the fine-grained nature of the carbonate particles embedded in the amorphous gel. The gel-derived material did not exhibit the well known endotherm due to the ferroelectric transition around 490 °C in the DTA curve. This result seems to indicate that although crystalline $PbTiO_3$ is observed by X-ray diffraction at 450 °C, the particle size is low so that the phase transformation is broadened off, whereas the $PbTiO_3$ powder after annealing at 950 °C for 48 h showed a reversible DTA peak around 490 °C, indicative of the coarsening of the particles and also the elimination of the non-thermodynamic defects present during their formation. The above interpretation of the TG–DTA results is supported by the X-ray powder diffraction data given below.

X-Ray diffraction. The sequence of reactions was studied by identifying the intermediate phases through X-ray diffraction, as shown in Fig. 3, after annealing the composite powder for various times at selected temperatures. The studies revealed the presence of intermediate phases appearing during the conversion of the carbonate–gel composite powder to tetragonal $PbTiO_3$.

The X-ray diffractogram of the as-prepared powder dried at 120 °C for 12 h [Fig. 3(a)] showed the presence of lead carbonate ($PbCO_3$) as the only crystalline phase. No titanium dioxide (TiO_2) is detected since it is in the amorphous form, as hydrated titania. Heat treatment of the powder at *ca.* 275 °C for 4 h results in the formation of PbO with tetragonal symmetry, whereas no reflections of TiO_2 (anatase or rutile) are observed [Fig. 3(b)].

As the calcination temperature is increased to 350 °C for 4 h [Fig. 3(c)], reflections of PbO (tetragonal) shifted to larger 2θ values, indicative of the decrease in *d*-spacings and cell parameters. This arises from the partial dissolution of TiO_2 in PbO (tetragonal) to form a solid solution, $(PbO \cdot zTiO_2)_{ss}$, where $z < 0.12$. This solid solution is known from the PbO–TiO_2 phase diagram.[13] The solid solubility arises from the partial replacement of Pb^{2+} by Ti^{4+} ions. The presence of the $PbO \cdot zTiO_2$ solid solution [designated herein as $(PbO)_{ss}$] could also be detected by chemical methods. PbO, present in the products of incomplete reaction, on dissolution in acetic acid showed the presence of titanium ions. The other phases are not soluble in weak acids such as acetic acid. Quantitative analysis showed that the maximum solubility of TiO_2 is *ca.* 9 mol%. The experimentally determined a_o and c_o values are plotted on the curve given by Matsuo *et al.*[14] and the estimated solubility of TiO_2 in PbO is *ca.* 8.2 mol%, which is in agreement with the chemical analysis results. The residue after acetic acid washing of the product contained a significant amount of Pb, as shown by chemical analysis. Since uncombined PbO is soluble in acetic acid, this should indicate a chemically combined form of PbO, such as $Pb_2Ti_2O_6$, $PbTiO_3$, $Pb_2Ti_2O_7$, *etc.* Takai *et al.*[15] assigned the reflections of $(PbO)_{ss}$ to arise from another form of lead titanate (designated as PT-I) which they considered as the first intermediate in the hydrothermal precipitation. Simultaneous to the shifts in the X-ray reflections of PbO is the appearance of additional reflections which could be matched with those of $Pb_2Ti_2O_6$.[16]

When the calcination temperature is increased to 375 °C, the intensities of the reflections from $Pb_2Ti_2O_6$ increase [Fig. 3(d)]. The formation of the defect pyrochlore $Pb_2Ti_2O_{7-\delta}$

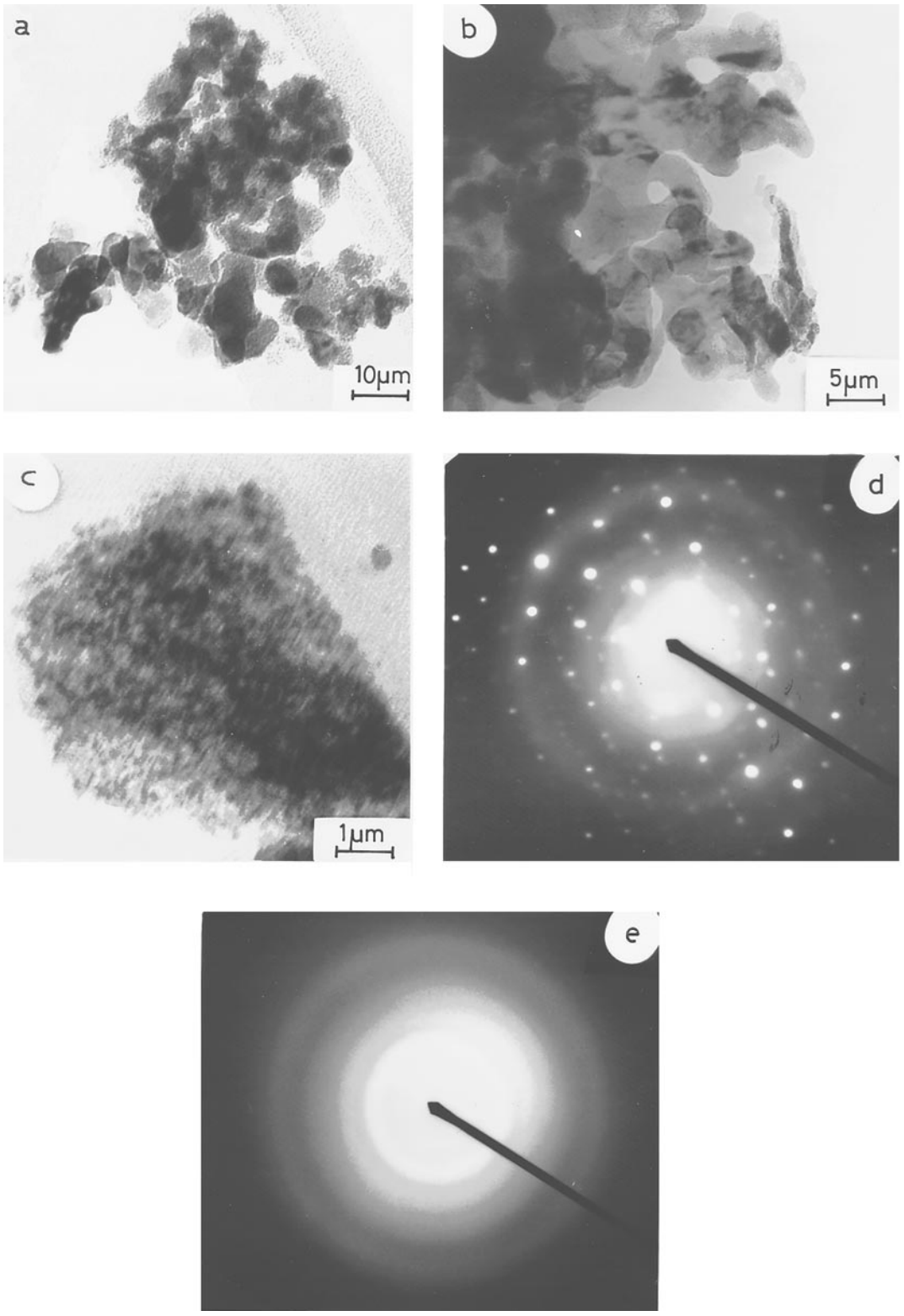

Fig. 1 (a)–(c) TEM images of a composite precipitate of $PbCO_3$ and hydrated titania under varying magnification; (d) the corresponding electron diffraction pattern and (e) the diffraction pattern of the amorphous titania hydrate gel

($\delta = 1$) from the borosilicate glass matrix containing lead oxide and titanium oxide has been reported.[17] This defect pyrochlore phase has the same composition as that of the perovskite, although it has a different crystal structure. $Pb_2Ti_2O_6$ is a metastable cubic phase with a lattice parameter of 10.44 Å. The X-ray diffraction lines observed in this study correspond to the characteristic pattern of the pyrochlore. The formation of the pyrochlore phase is attributed to its lower density in comparison to that of the perovskite phase. Thus, after calcination at 375 °C for 4 h, the X-ray reflections of the $PbO \cdot zTiO_2$ ($0 < z < 0.12$) solid solution and $Pb_2Ti_2O_6$ (defect pyrochlore) are observed.

Further calcination at 400 °C for 4 h [Fig. 3(e)] results in the evolution of the perovskite phase, in addition to $(PbO \cdot zTiO_2)_{ss}$ and the defect pyrochlore phase, $Pb_2Ti_2O_6$. Calcination at 450 °C for 4 h leads to the complete disappearance of $(PbO \cdot zTiO_2)_{ss}$ reflections accompanied by a drastic decrease in the intensities of the defect pyrochlore reflections and enhanced intensities for the perovskite reflections. Further annealing at 450 °C for extended periods (*ca.* 24 h) leads to the

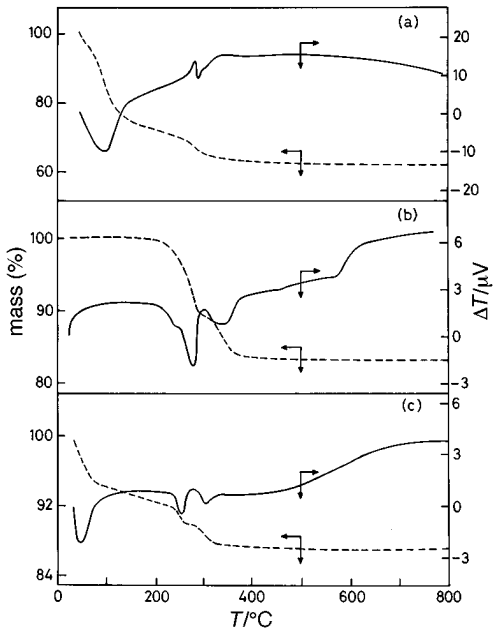

Fig. 2 TG–DTA data in air for (a) hydrated titania, (b) $PbCO_3$ and (c) a composite precipitate of $PbCO_3$ and hydrated titania

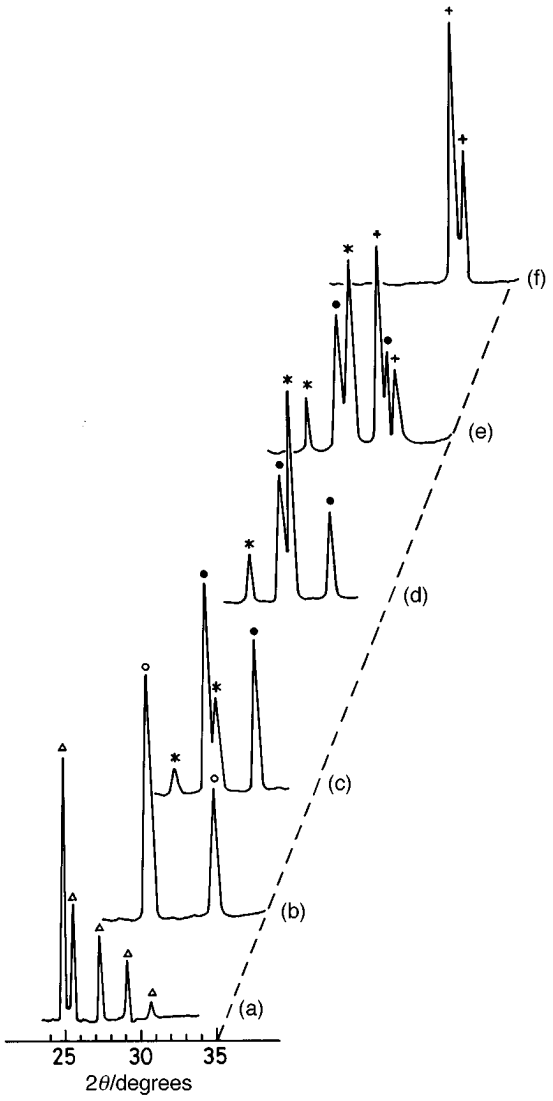

Fig. 3 X-Ray diffractograms [at (a) 120, (b) 275, (c) 350, (d) 375, (e) 400 and (f) 450 °C] showing the evolution of crystalline $PbTiO_3$ from the composite powder. Δ, $PbCO_3$; ○, PbO; ●, $(PbO\cdot zTiO_2)_{ss}$; *, $Pb_2Ti_2O_6$; +, $PbTiO_3$

formation of crystalline $PbTiO_3$ [Fig. 3(f)] with complete phase purity.

At no stages of calcination are the X-ray reflections corresponding to TiO_2 (anatase, rutile or brookite) observed, indicating that the amorphous phase of titania hydrate gives rise to $PbTiO_3$ through the formation of the intermediates $(PbO\cdot zTiO_2)_{ss}$ and $Pb_2Ti_2O_6$. The conversion of the defect pyrochlore to the perovskite is a continuous process with no mixed phase formation, as is evident from the X-ray diffractograms.

The powders prepared are highly reactive because of the low temperature of formation of the product. The product yield is nearly quantitative (≥99%). Highly crystalline and phase-pure powders are obtained.

The sequence of reactions in the preparation of $PbTiO_3$ can be formulated as follows:

$$TiO_2\cdot xH_2O \rightarrow TiO_2\cdot yH_2O + (x-y)H_2O \quad (1)$$

$$PbCO_3 \rightarrow PbO + CO_2 \quad (2)$$

$$PbO + zTiO_2\cdot yH_2O \rightarrow (PbO\cdot zTiO_2)_{ss} + yzH_2O \quad (3)$$

$$2PbO\cdot zTiO_2 + 2(1-z)TiO_2\cdot yH_2O \rightarrow Pb_2Ti_2O_6 + 2(1-z)yH_2O \quad (4)$$

$$Pb_2Ti_2O_6 \rightarrow 2PbTiO_3 \quad (5)$$

These steps differ completely from the solid–solid reaction starting from the constituent oxides PbO and TiO_2. The preparation of $PbTiO_3$ *via* the ceramic route is well known,[9–11,13] wherein the reaction between the crystalline phases takes place between 600 and 700 °C.

Under the dynamic conditions of thermal analysis, reactions (4) and (5) are not detectable in the DTA curves, as there are no large energy changes. Moreover, they are kinetically slower processes. This accounts for the necessity of annealing these composite powders for longer durations at temperatures between 350 and 450 °C.

Lead zirconium titanate (PZT)

Fig. 4 shows the TG–DTA curves of the as-prepared PZT powder after drying at 120 °C for 12 h. The sequence of reactions followed is the same as that observed for $PbTiO_3$. Three endotherms are observed, one at 65 °C (mass change 17%), the second around 249 °C and the third at 299 °C (combined mass change *ca.* 9%). In comparison, the DTA curve of the solid–solid reaction between PbO, TiO_2 and ZrO_2 shows an endotherm followed by an exotherm (Fig. 5). This pattern is essentially a composite of the two binary mixtures, as the formation of $PbTiO_3$ is exothermic in nature and that of $PbZrO_3$ is endothermic.[11] It can be seen that these reactions occur at much higher temperature in comparison to that observed for the present route. Thus, it is very clear that the nature of the reaction is completely different in the case of the product from carbonate–gel precipitation.

Fig. 6 shows the X-ray diffraction patterns of the powders calcined at different temperatures. The as-prepared powder

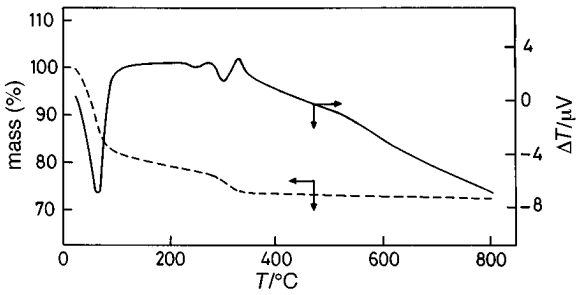

Fig. 4 TG–DTA data in air of the $Pb(Zr_{0.5},Ti_{0.5})O_3$ composite powder

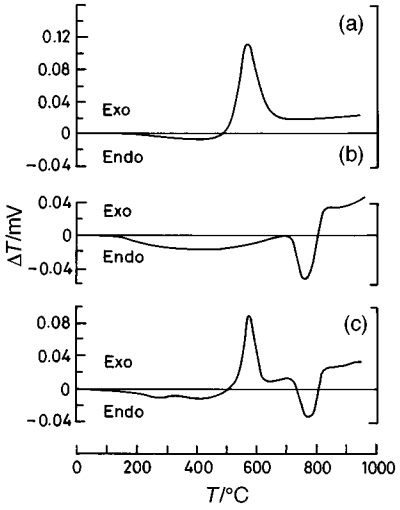

Fig. 5 DTA plots in air for (a) $PbO+TiO_2$, (b) $PbO+ZrO_2$ and (c) $PbO+0.5\ TiO_2+0.5\ ZrO_2$ mixtures (for more details see ref. 11)

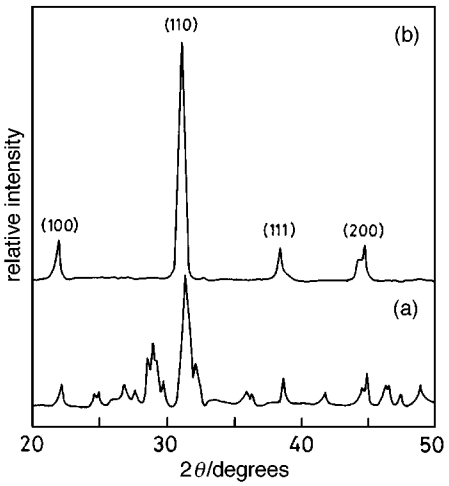

Fig. 6 X-Ray diffractograms of the $Pb(Zr_{0.5},Ti_{0.5})O_3$ composite precipitate calcined at (a) 400 and (b) 450 °C

(dried at 120 °C) showed the presence of the crystalline lead carbonate phase. Heat treatment at 400 °C for 4 h results in the formation of the mixed phase perovskite [$Pb(Zr_{0.5},Ti_{0.5})O_3$] (PZT), $(PbO)_{ss}$ and the defect pyrochlore phase [$Pb_2(Zr_{0.5},Ti_{0.5})_2O_6$]. Further annealing at 450 °C for 24 h results in the evolution of a crystalline perovskite with single-phase characteristics. Here again, no X-ray reflections corresponding to any of the crystalline phases of ZrO_2 and TiO_2 are observed at any stage of the thermal annealing.

Well defined acicular crystallites of PZT are obtained, as shown by the TEM image (Fig. 7). The particle size, calculated by the linear intercept method from the micrograph, is of the order of 0.3–1.2 μm.

The various compositions of PZT prepared are listed in Table 2. Depending upon the Zr/Ti ratios in the starting raw material, the final product formed will be tetragonal, rhombohedral or orthorhombic (pseudo-tetragonal). The cell dimensions of the product show systematic variations with changes in the Zr/Ti ratios (Fig. 8), with the end member, $PbZrO_3$, exhibiting a pseudo-tetragonal symmetry with cell parameters of $a'=4.158$ Å and $c'=4.108$ Å.

Conclusions

The carbonate–gel method results in composite powders with submicron particles of lead carbonate embedded within the amorphous hydrated titania or zirconia gel. The reaction

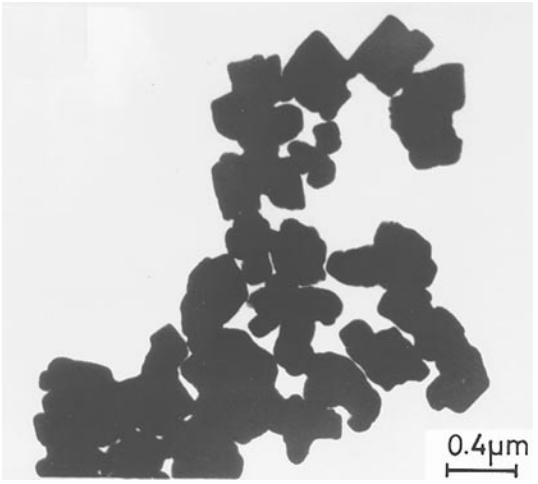

Fig. 7 TEM image of the $Pb(Zr_{0.5},Ti_{0.5})O_3$ powder indicating particle sizes of *ca.* 0.3–1.2 μm

Table 2 Compositions of PZT prepared

PZT compositions	phase symmetry
$PbZrO_3$	pseudo-tetragonal (orthorhombic)
$Pb(Zr_{0.8},Ti_{0.2})O_3$	rhombohedral
$Pb(Zr_{0.6},Ti_{0.4})O_3$	rhombohedral
$Pb(Zr_{0.5},Ti_{0.5})O_3$	rhombohedral
$Pb(Zr_{0.48},Ti_{0.52})O_3$	rhombohedral + tetragonal
$Pb(Zr_{0.45},Ti_{0.55})O_3$	tetragonal
$Pb(Zr_{0.4},Ti_{0.6})O_3$	tetragonal
$Pb(Zr_{0.2},Ti_{0.8})O_3$	tetragonal
$PbTiO_3$	tetragonal

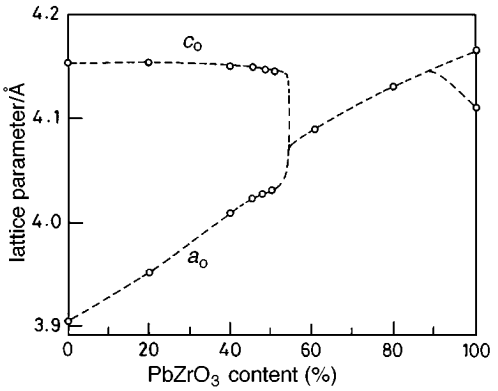

Fig. 8 Variation of lattice parameters with composition in the $PbTiO_3$–$PbZrO_3$ system

pathway followed by the composite powders is completely different from both the products of other wet chemcial processes and the solid–solid reaction between the binary oxides. The absence of a ferroelectric anomaly may be the result of the low particle size. Homogeneous mixed oxides of the perovskite series are obtained at relatively low temperatures in comparison to the ceramic processes, in which reactions go to completion only above 700 °C. The new method has the following advantages: (1) it is simple to adopt; (2) the raw materials involved are commonly available reagents; (3) highly reactive powders are obtained; (4) the product yield is >98%, and (5) highly phase-pure and crystalline products are obtained.

References

1 A. J. Moulson and J. M. Herbert, *Electroceramics*, Chapman and Hall, London, 1990.

2 P. P. Phule and S. H. Risbud, *J. Mater. Sci*., 1990, **25**, 1169.
3 *Better Ceramics Through Chemistry*, ed. C. J. Brinker, D. E. Clark and D.A. Ulrich, *Mater. Res. Soc. Symp. Proc*., North-Holland, Amsterdam, 1984, vol. 32.
4 L. M. Brown and K. S. Mazdiyasni, *J. Am. Ceram. Soc*., 1972, **55**, 541.
5 S. Kaneko and F. Imoto, *Bull. Chem. Soc. Jpn*., 1978, **51**, 1739.
6 A. N. Christensen and S. E. Ramussen, *Acta Chem. Scand*., 1963, **17**, 845.
7 R. Balachandran and T. R. N. Kutty, *Mater. Res. Bull*., 1984, **19**, 1479.
8 H. S. Gopalakrishnamurthy, M. Subbarao and T. R. N. Kutty, *J. Inorg. Nucl. Chem*., 1976, **38**, 417.
9 K. Aykan, *J. Am. Ceram. Soc*., 1968, **51**, 577.
10 J. Thomson, Jr., *Bull. Am. Ceram. Soc*., 1974, **53**, 421.
11 S. S. Chandratreya, R. M. Fulrath and J. A. Pask, *J. Am. Ceram. Soc*., 1981, **64**, 422.
12 T. R. N. Kutty, R. Vivekanandan and P. Murugaraj, *Mater. Chem. Phys*., 1988, **19**, 533.
13 B. Jaffe, W. R. Cook and J. Jaffe, *Piezoelectric Ceramics*, Academic Press, London, 1971.
14 Y. Matsuo and H. Sasaki, *J. Am. Ceram. Soc*., 1963, **46**, 409.
15 K. Takai, S. Shoji, H. Naito and A. Sawaoka, *Proc. 1st Int. Symp. Hydrothermal Reactions*, ed. Somiya, Association for Scientific Document Information Publications, Tokyo, 1983, p. 877.
16 JCPDS Powder Diffraction File, Inorganic Volume, card no. 26–142.
17 F. W. Martin, *Phys. Chem. Glasses*, 1965, **6**, 143.

Paper 6/06449C; *Received* 18*th September*, 1996